Rhizosphere microbiome mediates systemic root metabolite exudation by root-to-root signaling

Elisa Korenblum[a], Yonghui Dong[a], Jedrzej Szymanski[b], Sayantan Panda[a], Adam Jozwiak[a], Hassan Massalha[a], Sagit Meir[a], Ilana Rogachev[a], and Asaph Aharoni[a,1]

[a]Plant and Environmental Science Department, Weizmann Institute of Science, Rehovot 7610001, Israel; and [b]Department of Molecular Genetics, Leibniz Institute of Plant Genetics and Crop Plant Research, OT Gatersleben, Corrensstraße 3, D-06466 Seeland, Germany

Edited by Jeffery L. Dangl, University of North Carolina at Chapel Hill, Chapel Hill, NC, and approved January 3, 2020 (received for review July 15, 2019)

Microbial communities associated with roots confer specific functions to their hosts, thereby modulating plant growth, health, and productivity. Yet, seminal questions remain largely unaddressed including whether and how the rhizosphere microbiome modulates root metabolism and exudation and, consequently, how plants fine tune this complex belowground web of interactions. Here we show that, through a process termed systemically induced root exudation of metabolites (SIREM), different microbial communities induce specific systemic changes in tomato root exudation. For instance, systemic exudation of acylsugars secondary metabolites is triggered by local colonization of bacteria affiliated with the genus *Bacillus*. Moreover, both leaf and systemic root metabolomes and transcriptomes change according to the rhizosphere microbial community structure. Analysis of the systemic root metabolome points to glycosylated azelaic acid as a potential microbiome-induced signaling molecule that is subsequently exuded as free azelaic acid. Our results demonstrate that rhizosphere microbiome assembly drives the SIREM process at the molecular and chemical levels. It highlights a thus-far unexplored long-distance signaling phenomenon that may regulate soil conditioning.

root exudation | microbiome | metabolomics | long-distance signaling

Living within a composite environment, plants interact with specific soil microorganisms that inhabit their root vicinity, called the rhizosphere (1). The rhizosphere is one of the most complex ecosystems on earth, considered a hotspot fostering millions of microbial cells. The microbial diversity in the rhizosphere changes according to plant developmental stages, genotypes, and soil environment (2–5). The interactions of microorganisms that coexist in the rhizosphere are dynamic, and fluctuations of metabolites exuded by plant roots help shape the composition of the root microbiota (6).

Root exudation is a key mechanism by which plants interact with soil microbes (7). By changing the root microbiota, root exudates play an important role in plant–soil feedback, governing plants' survival under abiotic and biotic stresses (8–10). Roots exude a diverse repertoire of metabolites, including up to 10–50% of the plants' fixed carbon (11–13). The dynamics of root growth and exudation processes change the chemical composition of the rhizosphere in space and time. Most studies reporting root exudate composition were performed with sterile hydroponic systems to avoid microbial degradation of plant metabolites (14). For instance, the model plant *Arabidopsis thaliana* grown in hydroponics exuded a hundred different metabolites representing several chemical classes (15). This metabolic diversity suggests an intricate plant chemical language that mediates uncountable rhizosphere interactions (11, 16, 17). For example, coumarins and benzoxazinoids are known secondary metabolites exuded by roots and play a role in shaping the root microbiota (9, 18); even small changes in the microbial communities' structure might result in large alterations of host phenotypes (19).

The Rosetta Stone of rhizosphere interactions is still largely unknown; cryptic multimolecular signals exist in the rhizosphere. To understand the complex nature of rhizosphere processes and plant–soil feedback, disentangling internal and external signals that influence plant–microbial relationships is crucial. Many external signals initially reach in a likely localized manner to a particular position in the root system. Thus, systemic, long-distance signaling between different parts of the root system primes plant responses to potential environmental challenges and is crucial for plant fitness. Root systemic responses were mostly studied in the context of plant pathogen resistance or nutrition. Nitrogen acquisition and autoregulation of nodulation are two established systemic responses functioning among parts of the same root system (20, 21). In nodulation, for example, nodule formation acts as a local elicitor and triggers a distinct systemic response as fewer nodules are formed in distal parts. Interestingly, in both cases, the initial signal from roots (i.e., a secreted peptide) moves to the shoot and a second signal subsequently descends back to the root to transduce the signal. Conversely, in the field of plant–microbial interactions, which mostly regards the microbial counterpart as pathogenic or beneficial, that either elicits plant defense or protection, "systemic" is usually connoted as a general response (i.e., resistance is observed in local and distal parts) (22).

In nature, specifically in the rhizosphere, plants are constantly challenged by thousands of different microbial populations,

Significance

Root exudation of metabolites is an important mediator of plant interactions with soil microbes. Here we demonstrate that the tomato rhizosphere microbiome affects the chemical composition of root exudation through a systemic root–root signaling mechanism. We termed this process SIREM (systemically induced root exudation of metabolites) and showed that specific microbial colonization of the "local-side" root modulates the exudate composition at the "systemic side." For example, *Bacillus subtilis* modulates systemic exudation of the renowned acylsugars insecticides. We also discovered that glycosylated azelaic acid is microbiome induced and might act in SIREM. The results suggest that microbiome-reprogrammed systemic root exudation promotes soil conditioning and pave the way for deeper understanding of how microbiota modulate root metabolism and secretion.

Author contributions: E.K. and A.A. designed research; E.K., S.P., A.J., H.M., and S.M. performed research; E.K., Y.D., J.S., and I.R. analyzed data; and E.K. and A.A. wrote the paper.

The authors declare no competing interest.

This article is a PNAS Direct Submission.

Published under the PNAS license.

Data deposition: The raw 16S rRNA amplicon-seq and RNA-seq reads reported in this paper have been deposited to National Center for Biotechnology Information (NCBI Short Read Archive under Project PRJNA602077). The metabolomics data were submitted to MetaboLights, https://www.ebi.ac.uk/metabolights/ (accession no. MTBLS1458).

[1]To whom correspondence may be addressed. Email: asaph.aharoni@weizmann.ac.il.

This article contains supporting information online at https://www.pnas.org/lookup/suppl/doi:10.1073/pnas.1912130117/-/DCSupplemental.

First published February 3, 2020.

Downloaded at University of Manitoba Libraries on April 6, 2020

including commensals, pathogens, and symbionts. Yet, whether and how this complex rhizosphere microbiota affects root metabolite composition and exudation have not yet been addressed (23, 24). We hypothesized that rhizosphere microbiota induces several host systemic signals that trigger distal metabolic reprogramming and consequently differential root exudation. Our findings underline the phenomenon of systemically induced root exudation of metabolites (SIREM), which is modulated by local microbial colonization on roots. We first examined if soil microbial communities affect the chemical composition of SIREM-induced exudates by the use of a tomato split-root hydroponic system with one root side treated with different microbial communities. Following metabolic profiling of systemic plant tissues, we found that azelaic acid (AzA) glycoside accumulates in "systemic-side" roots after microbiome treatment. The AzA aglycone is known to accumulate in plants during pathogen attack, but only in locally infected leaves (25). Thus, we pharmacologically challenged split-root plants with AzA to test if AzA or AzA derivatives are plant internal signals that lead to SIREM. We also selected bacterial candidates from the root microbiome that induce specific metabolic changes in SIREM to establish a causal link of root bacterial colonization and root exudation. In summary, we present SIREM, an unexplored phenomenon mediating root exudation that triggers chemical diversification in the rhizosphere and is dependent on the root microbial community composition.

Results

Establishing Variable Tomato Rhizosphere Microbiomes in a Split-Root Hydroponic Set-Up. In an effort to test the effect of soil microbial communities on the chemical composition of roots and exudates released from uncolonized roots, we established a tomato split-root hydroponic set-up (Fig. 1*A*). The uncolonized root side (termed "systemic side") was maintained under axenic conditions for exudate collection. Split-root seedlings (14 d after germination) were transferred to hydroponic vials (Fig. 1*A* and *SI Appendix*, Fig. S1*A*) set inside UV-sterilized plastic boxes. To compare the effect of rhizosphere microbial diversity on root exudation, one side of the split-root hydroponic system (termed "local side") was inoculated with different soil microbial communities, generated by using a "dilution-to-extinction" approach (26). We prepared three soil suspensions of serially diluted (10^{-2}-, 10^{-4}-, and 10^{-6}-fold diluted) natural sandy-loam soil into an autoclaved soil solution (AS), obtaining root microbiomes with high, medium, and low diversity levels (termed HD, MD, and LD, respectively). AS-treated plants served as a control samples. We profiled the rhizosphere bacterial communities from three to six biological replicates (each replicate consisted of the rhizosphere, i.e., soil attached to roots, of three pooled plants) at the local side 7 d after root inoculation (28 d after germination, Fig. 1*A* and *SI Appendix*, Fig. S1*B*). Incubation time in the hydroponic set-up was based on oxygen availability in the hydroponic vials (*SI Appendix*, Fig. S1*C*) and earlier reports demonstrating that microbiome establishment on roots is detectable in a short period of time (9).

Given the manipulation of soil microbial community using a "dilution-to-extinction" approach, we anticipated the three rhizosphere microbiomes to present initial different microbial cell numbers and following 7 d of incubation a gradual decrease in species richness (26). Indeed, results from the 16S rRNA amplicon sequencing (Dataset S1 *A*–*C*) revealed that the three bacterial communities colonizing local-side roots were markedly different, disclosing a significant decrease in richness and/or diversity values (ANOVA, $P < 0.01$) (Fig. 1*B* and *SI Appendix*, Fig. S3*A*). According to nonmetric multidimensional scaling (NMDS) plots, bacterial community composition differed among the rhizosphere microbiomes (*SI Appendix*, Fig. S4). Proteobacteria significantly changed but were predominant in all samples while operational taxonomic units (OTUs) related to the phylum Bacteroidetes were enriched on higher diversity samples. Firmicutes were highly enriched in the MD and LD samples (Fig. 1*C* and *SI Appendix*, Figs. S3*B* and S4). Interestingly, at all taxonomic levels, all phyla up to genera that occurred in HD samples, also occurred in the MD and LD samples; however, their relative abundances changed. For instance, the four major bacterial taxa classified at the order level (each representing more than 10% of total reads) exhibited significant differential abundance among the root microbiomes (Kruskal–Wallis, false discovery rate [FDR] <0.05, *SI Appendix*, Fig. S4*B*). We detected a significant decrease in OTUs related to Pseudomonadales and Burkholderiales as microbial diversity

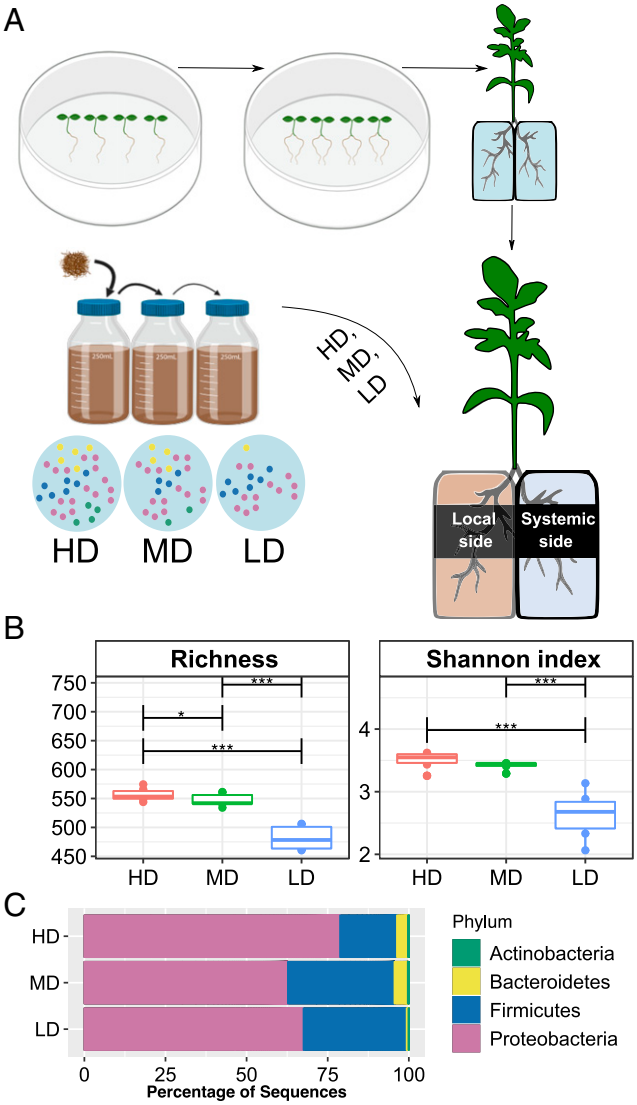

Fig. 1. Linking local-side root microbiome diversity to the chemical composition of systemic root exudation. (*A*) Schematic representation of the split-root hydroponics experimental design. Local-side roots of the split-root set-up were inoculated with soil microbiome, established using the dilution-to-extinction approach; HD, MD, or LD diversity microbiomes and exudate samples were collected from the systemic side. (*B*) Alpha diversity indices of root microbiomes (local side) measured 7 d postinoculation. Number of species (richness) or Shannon index gradually decreased among HD, MD, LD microbiomes (asterisks denote difference in alpha diversity indices, $*P < 0.05$, $***P < 0.0005$, ANOVA followed by Tukey's honestly significant difference (HSD) post hoc multiple comparison). (*C*) Bar plots of relative abundances of the top four phyla in each root microbiome (HD, MD, and LD) after 7 d of inoculation. Data are the average of six biological replicates. OTU abundance (97% similarity) and assigned taxonomic classifications used to construct this panel can be found in Dataset S1C. The bacterial relative abundance displayed at the phylum level for all individual samples can be found in *SI Appendix*, Fig. S3*B*.

Downloaded at University of Manitoba Libraries on April 6, 2020

decreased, although a significant gradual increase in OTUs related to Bacillales and Enterobacteriales (Kruskal–Wallis, FDR <0.05). After 7 d of microbiome treatment, the plants exhibited similar shoot and root weight as compared to AS controls and untreated plants (i.e., grown in sterile water only, *SI Appendix*, Fig. S5*A*).

Local Rhizosphere Microbiome Changes Root Exudation of Secondary Metabolites in Distal Parts of the Root System. Following 7 d of microbiome treatment, root exudates accumulating in the systemic side were subjected to metabolite profiling using high-resolution mass spectrometry. In this first experiment, systemic-side exudates of three individual plants were pooled and analyzed for differential semipolar metabolites. Notably, following microbiome treatments of the local side, systemic-side roots displayed substantial changes in exudate composition (*SI Appendix*, Fig. S6*A*). Metabolomics data showed that 569 masses (53.3%, electrospray negative ionization mode, ES^- mode) to 1,119 masses (75.4%, electrospray positive ionization mode, ES^+ mode) of the total mass features were significantly modulated by one of the three microbiomes (twofold change cutoff between one of the microbiome treatments and AS controls; $P < 0.05$, one-way ANOVA followed by multiple comparisons with FDR correction). From these mass features, we detected a total of 115 metabolites that were significantly enriched or depleted in the systemic side that was modulated by the local-side root microbiome (Fig. 2*A* and Dataset S2 *A*–*C*). Most of these

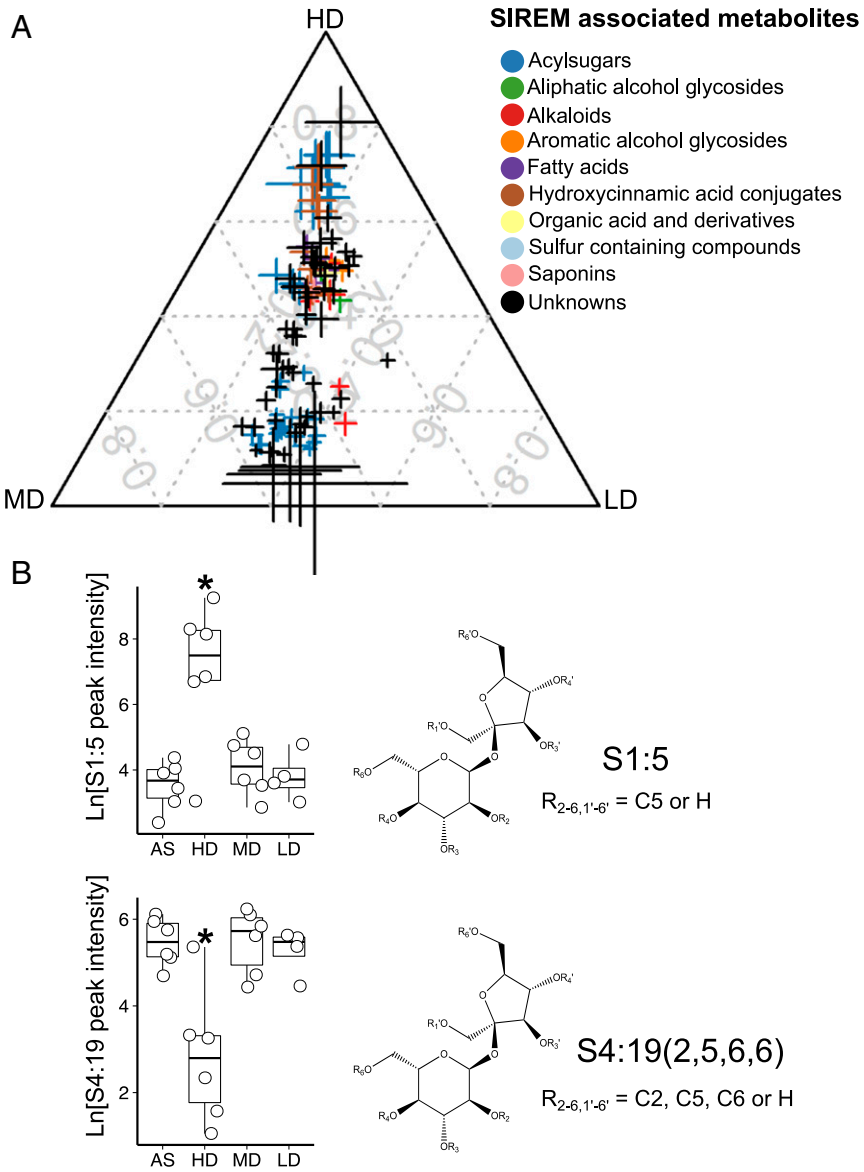

Fig. 2. SIREM represents a root–root long-distance signaling that results in systemic exudation of various classes of metabolites. (*A*) Ternary plot of SIREM-induced metabolites differentially enriched in HD-, MD-, or LD-treated plants as compared to AS-control plants. Each data point represents a metabolite enriched in the systemic-side exudate associated with a microbiome treatment in the local-side root ($n = 5$ to 6, FDR <0.05, fold change >2). Data point size denotes the sum of fold change (square root transformed) of one metabolite in HD-, MD-, or LD-treated samples as compared to the AS controls. Data point position indicates the percent of each metabolite present in each group (i.e., HD, MD, LD). Color codes represent the metabolite chemical class. The metabolite annotation data and numerical values used to construct the ternary plot can be found in Datasets S2 *A* and *C*, respectively. (*B*) Root microbiome modulation of acylsucrose acylations in SIREM. Boxplots of peak intensities (natural log transformed) of representative acylsucroses that were HD-enriched (C5 acylsucrose; S1:5) and HD-depleted [acylsucrose with different acyl chains, S4:19 (2, 5, 6, 6)]. Asterisks above boxes indicate significant difference tested by ANOVA performed with Tukey's HSD test ($n = 5$ to 6, FDR <0.05). Structures of C5 acylsucroses and S4:19 (2, 5, 6, 6) are depicted on the *Right* side of the boxplots.

Downloaded at University of Manitoba Libraries on April 6, 2020

metabolites (93 in total) were modulated specifically by one of the three root microbiome treatments (Dataset S2*C*). We next putatively annotated 56 metabolites (confidence levels in metabolite annotation for all annotated compounds from this study are indicated in Dataset S2*A*). These metabolites represented diverse chemistries, including acylsugars, aliphatic and aromatic alcohol diglycosides, fatty acids, hydroxycinnamic acid conjugates, organic acid derivatives, sulfur-containing compounds, steroidal glycoalkaloids (SGAs), and steroidal saponins (SSAs).

We discovered that metabolites exuded following microbiome treatments predominantly belonged to the acylsugars class. Acylsugars produced by tomato and other members of the Solanaceae family typically consist of either glucose or sucrose backbones esterified with three to four acyl chains, each containing 2 to 12 carbons. However, to date, this group of secondary metabolites was merely reported to accumulate specifically in the tip cell of leaf glandular trichomes (27). Remarkably, acylsucrose (26 metabolites) and acylglucose [specifically G2:12 (6, 6); seven isomers; "G" indicates a glucose backbone, while "2:12" denotes the presence of two acyl chains of 6 carbons that decorate the sugar moiety] were exuded through the systemic-side roots. The sugar moiety and the length of the acyl chains differed according to the root microbiome composition. Hence, HD-treatment exuded significantly higher amounts of acylsucroses with C5 acyl chains only (S1:5, S2:10, and S3:15; "S" indicates sucrose; *SI Appendix*, Fig. S7 *A* and *B* and Dataset S2 *A–C*). The metabolite S1:5 isomer 3 (Fig. 2*B* and Dataset S2*C*) was the most abundant acylsucrose in exudates of HD-treated plants. Previously, this metabolite was detected only in an in vitro reaction using sucrose and iC5-CoA as substrates of the SlASAT1 enzyme (Solyc12g006330) (28) but not in planta. Furthermore, mono-, di-, and triacyl sugars decorated with only C5 acyl chains are rare in the trichomes of M82 (29), the tomato cultivar used in our experiments. Additionally, acylglucoses were not found in tomato glandular trichomes (29, 30). Interestingly, we detected both acylsucroses and acylglucoses with acyl groups of varying lengths in tomato exudates; these were significantly reduced in the HD-treated plants (Fig. 2*B* and Dataset S2 *A–C*). The number and type of acyl chains and sugar backbone may determine specific functional roles of acylsugars in plant interactions (31).

The second predominant chemical class in exudates was hydroxycinnamic acid conjugates (Fig. 2*A* and Dataset S2 *A–C*). HD-treated plants exuded hydroxycinnamic acid amides (HCAAs) conjugated to tyramine or octopamine. These metabolites were found in numerous plants and recognized as defensive molecules in leaves triggered upon pathogen attack (32). As for acylsugars, HCAAs were not reported in root exudates of any other plant species to date. On the other hand, ferulic acid glycosides were previously detected in *Arabidopsis* exudates grown in sterile conditions (33). Here, we detected ferulic acid hexoses that were reduced in LD-treated plant exudates (Dataset S2 *A–C*). In the same way, the SGA hydroxytomatine accumulated in exudates of HD-treated plants while dehydrotomatine was reduced in LD-treated plants. These specific SGAs are typically found in tomato leaves and fruit (29, 34). Moreover, fatty acid derivatives, four oxylipin isomers (trihydroxy-octadecanoic acid, Dataset S2 *A–C*) and azelaic acid were also enriched in exudates from HD-treated plants (Dataset S2 *A–C*). These metabolites were associated with leaves' systemic defense response (35), but these were not reported previously to occur in root exudation. Altogether, the observed enrichment and suppression of metabolites in these experiments supported our primary hypothesis that rhizosphere microbiome modulates the chemical composition of exudates in a systemic manner. We termed this long-distance signaling between parts of a single root system as systemically induced root exudation of metabolites (SIREM).

Rhizosphere Microbiome Induces Systemic Metabolic Changes in Roots and Shoots. We next analyzed the metabolic changes of shoot and root tissues harvested from plants grown and treated in the same experimental set-up described above. A total of 172 semipolar metabolites were significantly altered in tomato tissues following microbiome treatment (twofold change cutoff between one of the microbiome treatments and the AS controls; $P < 0.05$, one-way ANOVA followed by multiple comparisons with FDR correction). The rhizosphere microbiome induced systemic tissue-specific responses (Dataset S2 *D* and *E*) as most of the metabolites enrichment or suppression were specific to plant sample type. Rhizosphere microbiome treatment at the local side modulated 116 and 56 metabolites in the systemic-side shoot and root tissues (Dataset S2 *D* and *E*), respectively. We annotated three amino acids and 20 secondary metabolites detected in shoots into seven chemical classes: acylsugars, alkaloids, anthocyanins, aromatic alcohols, flavonols, hormones, and hydroxycinnamic acid conjugates (*SI Appendix*, Fig. S8 *A–D* and Dataset S2*D*). HD treatment induced an increase of hydroxycinnamic acid conjugates (5 out of 6; *SI Appendix*, Fig. S8*C*) in tomato shoots and, MD-treated plants showed a lower level of flavonols (*SI Appendix*, Fig. S8*D*). In the systemic-side root, we annotated 10 out of the 56 metabolites (Fig. 3*A* and Dataset S2*E*). Notably, two organic acid glycosides, azelaic acid (di)hexose (AzA-Hex) and pimelic acid hexose (PIM-Hex), increased in the systemic-side roots of both HD- and LD-treated plants (Fig. 3*B*). In *Arabidopsis*, AzA induces systemic acquired resistance (SAR) (36) and was suggested to be a SAR mobile signal either as an AzA aglycone or as a derivative (37, 38). Dicarboxylic acids such as AzA and PIM are products of the galactolipids oxidation pathway (39).

Azelaic Acid Induced Systemic Changes in Shoot and Exudates. The discovery of root microbiome-induced AzA and PIM glycosides prompted us to investigate whether: 1) AzA can be transported systemically from the local-side root to systemic tissues (i.e., shoot and root) and whether 2) local-side AzA application can elicit SIREM. Application of 1 mM AzA to the local-side root resulted in the detection of AzA-Hex in the systemic tissues (both shoot and root) and its aglycone in systemic-side exudates (*SI Appendix*, Fig. S9). Moreover, we found that AzA induces systemic changes to metabolic profiles of shoots and systemic-side exudates (*SI Appendix*, Fig. S10*A*). Besides AzA-Hex, AzA local application affected the accumulation of the PIM aglycone in the systemic-side root (*SI Appendix*, Fig. S10*B*). PIM and feruloyltyramine were highly enriched in shoots of AzA-treated plants (FDR <0.05; *SI Appendix*, Fig. S10*B*). In addition, AzA increased the systemic root secretion of the SGA α-tomatine (*SI Appendix*, Fig. S10*B*). The results suggested that AzA-Hex is either transported to systemic tissues or accumulated in them and possibly induces specific plant metabolic reprogramming as part of the SIREM process.

SIREM Involves Significant Changes in Primary Metabolites According to Root Microbiome Composition. We employed the split-root system to profile polar metabolites (i.e., largely primary metabolites) in systemic tissues (i.e., in shoot, roots, and exudates) following microbiome application (HD, MD, and LD treatments) using gas chromatography-mass spectrometry (GC-MS). In contrast to secondary metabolites discussed above, root microbiome had no effect on primary metabolites detected in systemic-side roots and shoots (Dataset S3 *B* and *C*). We also characterized SIREM by analyzing the repertoire of primary metabolites (Dataset S3*A*). Based on our GC-MS analysis, tomato exudates typically contain sugars, sugar alcohols, amino acids, fatty acids, and organic acids. Only exudates of LD-treated plants displayed altered primary metabolites; while fructose and myoinositol were enriched in the LD exudates, benzoic acid, arabinose, and glucose were significantly depleted (*SI Appendix*, Fig. S11).

Downloaded at University of Manitoba Libraries on April 6, 2020

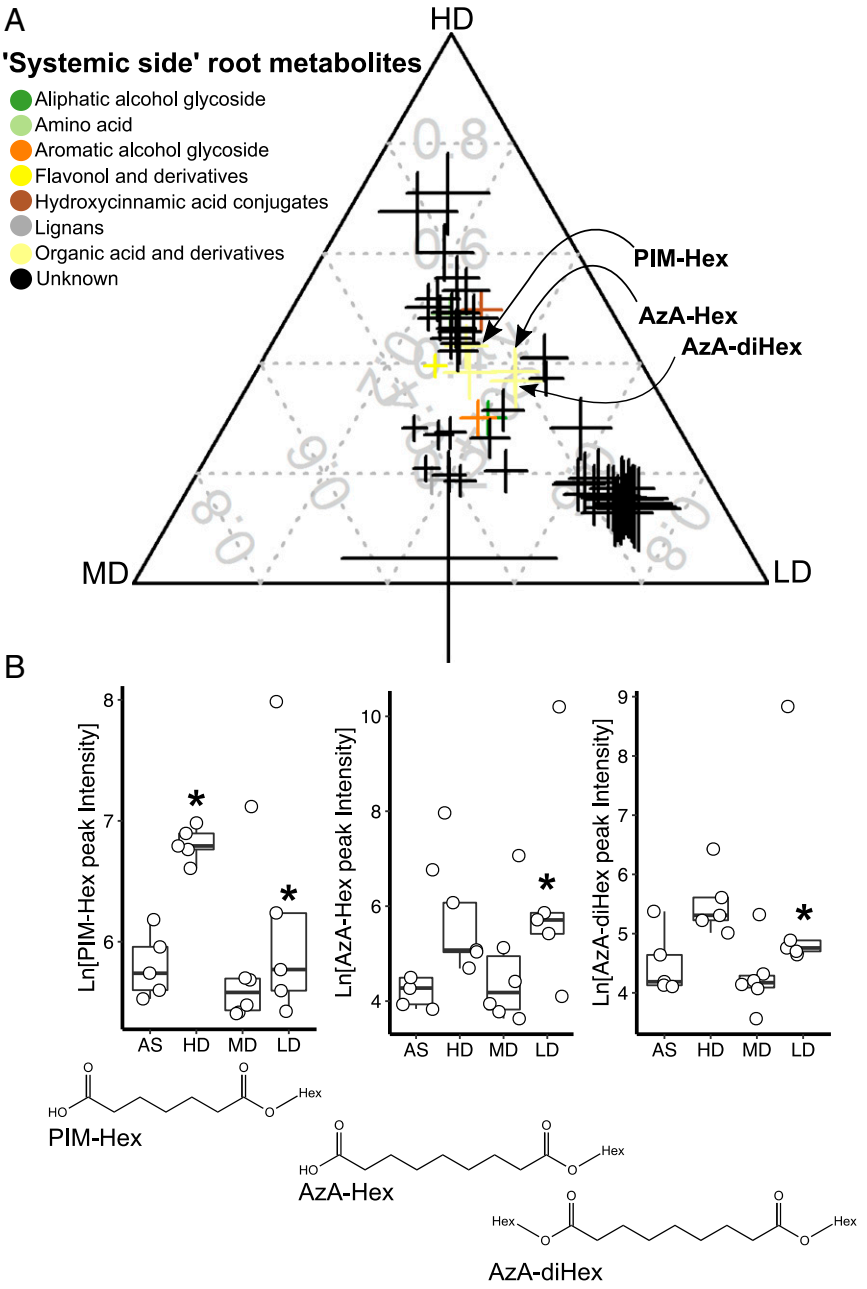

Fig. 3. Glycosylated forms of azelaic and pimelic acids accumulate in the systemic root side upon SIREM induction. (*A*) Ternary plot of metabolites differentially enriched in the systemic-side root tissue of HD-, MD-, or LD-treated plants as compared to AS-control plants. Each data point represents a metabolite enriched in the systemic-side root associated with a microbiome treatment in the local-side root (n = 5 to 6, FDR <0.05, fold change >2). Data point size denotes the sum of fold change (square root transformed) of one metabolite in HD-, MD-, or LD-treated samples as compared to the AS controls. Data point position indicates the percent of each metabolite present in each group (i.e., HD, MD, LD). Color codes represent the metabolite chemical class. Data points of azelaic acid dihexose (AzA-(di)Hex) and pimelic acid hexose (PIM-Hex) are highlighted. The metabolite annotation data and the numerical values used to construct the ternary plot can be found in Dataset S2 *A* and *E*, respectively. (*B*) Root microbiome induced of the accumulation of azelaic and pimelic acids glycosides in systemic-side roots. AzA-(di)Hex and PIM-Hex peak intensities (natural log transformed) are represented in boxplots. Asterisks above boxes indicate significant difference tested by ANOVA performed with Tukey's HSD test (n = 5 to 6, FDR <0.05). Structures of AzA-(di)Hex and PIM-Hex are depicted below the corresponding boxplots.

Spatial Mapping of SIREM-Associated Metabolites Reveals Their Accumulation in Exclusive Root Parts. We employed matrix-assisted laser desorption/ionization-mass spectrometry imaging (MALDI-MSI) to monitor the spatial distribution of metabolites detected in earlier experiments. The acquired MALDI-MSI results provide visual evidence for precise metabolite accumulation in particular zones of the entire root system. Plants were grown on a glass slide covered with a thin agar layer containing MS medium containing 1% soil suspension (representing a high-diversity microbiome). SIREM-related metabolites detected by LC-MS (Dataset S2*A*) were used to search for specific mass signals in our MALDI-MSI data. It is important to note that due to technical limitations (i.e., practical difficulties to establish the split root system on glass slides covered with MS agar), MALDI-MSI analysis was performed on the entire root system, while LC-MS analysis was conducted on systemic-side root extracts. Interestingly, while acylsucrose S1:5

Downloaded at University of Manitoba Libraries on April 6, 2020

(found earlier as HD enriched in exudates) was localized to the lateral root tips, S4:19 (HD depleted in exudates) were predominantly distributed along the hairs of the main root (Fig. 4 *A–D*). Similarly, SGAs (Fig. 4 *E–L*), lignans, hydroxycinnamic acids, and organic acids (*SI Appendix*, Fig. S12 *B–F*) appeared to accumulate in distinctive and highly localized root domains. Together, these results demonstrate that metabolites are localized to specific and distinct regions (e.g., tips of lateral roots or root hairs) and not equally distributed in the root system.

Systemic Modulation of the Plant Transcriptome by Root Microbiome Colonization. We anticipated that SIREM involves systemic modulation of gene expression in systemic-side root and shoot tissues. Thus, we employed the split-root system to check differential gene expression in systemic tissues following microbiome treatment of the local side. In this experiment, RNA samples extracted from shoots and systemic-side roots were subjected to transcriptome analysis. A total of 408 transcripts were differentially expressed when comparing HD, MD, or LD to AS-treated plants (log2-fold change >1, FDR <0.1; Dataset S4 *A* and *B*). The majority of genes in shoots (188 out of 323) and systemic-side roots (67 out of 92) were repressed (*SI Appendix*, Fig. S13); 7 genes were similarly expressed in shoots and systemic-side roots (*SI Appendix*, Fig. S13 *A* and *B*). Repressed genes (*SI Appendix*, Fig. S13 *D* and *F* and Dataset S4*C*) in both systemic tissues were enriched in carbohydrate metabolism (25 genes, Gene Ontology [GO]:0005975), and 5 genes were subcategorized into cell wall metabolism (GO:0010383). In systemic-side roots of HD-treated plants, multiple transcripts for xyloglucan endotransglucosylase (Solyc03g093080, Solyc05g005680, Solyc08g005610) were down-regulated. While genes related to riboflavin biosynthesis (Solyc04g008990) and calcium signaling (Solyc03g080080) were also down-regulated in systemic-side roots of HD-treated plants; additional genes related to these functions (riboflavin biosynthesis [Solyc07g054190] and calcium signaling [Solyc04g058160]) were up-regulated in MD- and LD-treated plants. Interestingly, down-regulation of cell wall-related genes and up-regulation of redox homeostasis genes is typically associated with SAR (40–42). A set of induced genes from systemic parts of plants represented oxidoreductase activity (24 genes, GO:0016491, Dataset S4*D*). Genes related to biosynthesis of oxylipins (9-lipoxygenases [Solyc08g029000, Solyc01g099190]) were highly up-regulated in shoots of MD-treated plants. Oxylipins are known modulators of local and systemic plant defense (35). We found oxylipins metabolites in exudates, but only from HD-treated plants. In addition, genes encoding pathogenesis-related (PR) proteins (PR5 [Solyc08g080670, Solyc04g081550]) were up-regulated in shoots of all microbiome-treated plants. PR proteins are well-known molecular markers for SAR in leaves that are distant from the infection site (40). Hence, it appeared that SAR and SIREM share similar transcriptome changes but are not identical processes (Fig. 5*A* and Dataset S4*E*).

Specific Root Microbial Populations Drive Transcriptional and Metabolite Reprogramming Resulting in Exudation of Particular Metabolites in SIREM. We integrated the various datasets acquired by this stage to identify coordinated changes in transcriptome, tissue, and exudation metabolic profiles and microbiome composition in the

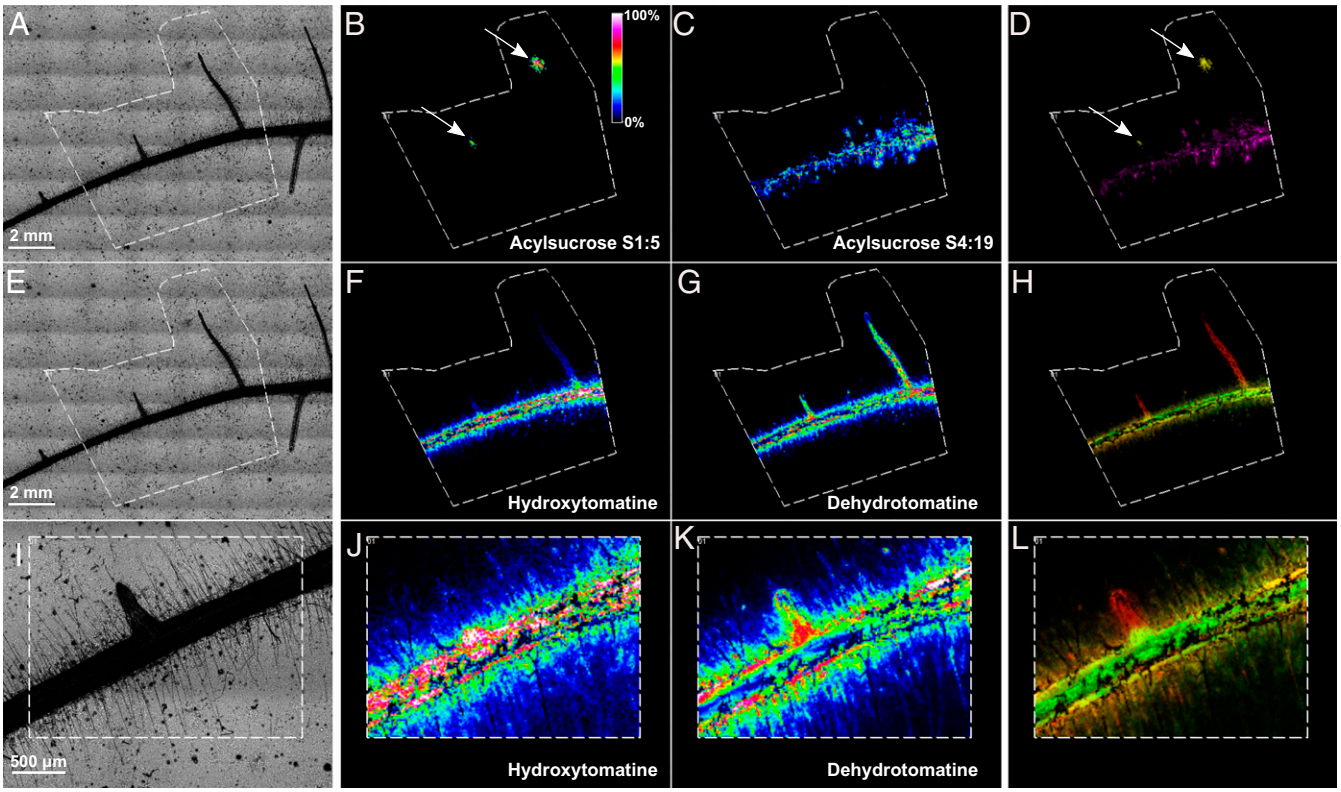

Fig. 4. Acylsugars and SGAs exuded in SIREM are localized in specific and varying root regions. (*A*, *E*, and *I*) Optical images of the tomato root used for MALDI-MSI analysis. The white broken line marks the region analyzed by MALDI-MSI. (*B*) MALDI-MSI of acylsucrose S1:5, *m/z* 427.18 ± 0.01 Da; (*C*) acylsucrose S4:19, *m/z* 665.33 ± 0.01 Da; (*F* and *J*) hydroxytomatine, *m/z* 1050.54 ± 0.01 Da; and (*G* and *K*) dehydrotomatine, *m/z* 1032.54 ± 0.01 Da. The intensity of spectra representing each metabolite is visualized in false color. (*D*, *H*, and *L*) Overlap of false color MALDI-MSI images of acylsucroses or SGAs. Arrows in *B* and *D* point to the specific accumulation of the S1:5 in the tip of lateral roots. The two representative SGAs are distributed along the main roots, while dehydrotomatine was also distributed along the lateral roots.

Downloaded at University of Manitoba Libraries on April 6, 2020

course of SIREM. A cross-validated self-organizing map (SOM) analysis was performed based on a four-by-four matrix that classified all variables in 16 clusters (i.e., SOM cells; each cluster represented a pattern of systematic changes shared between two or more variables independently of their class [i.e., transcript, metabolite, or OTU]). We then visualized these patterns using boxplots (Fig. 5*B*, *SI Appendix*, Fig. S14, and Dataset S5). The analysis revealed that a number of transcript and metabolic changes were related to the abundance of specific taxa in the soil microbiome, while others correlated with genetically diverse bacterial populations. We focused on 3 SOM clusters related to the major bacterial taxa found in the local-root microbiomes. In cluster 7, OTUs closely related to Pseudomonadales (85.36% of OTUs in cluster 7, Fisher exact test, $P < 0.00001$) were associated specifically with PIM-Hex accumulation in roots. In addition, Pseudomonadales-related OTUs (cluster 11) correlated with systemic exudation of two isomers of ferulic acid dihexose and additional yet unknown molecules. The third cluster (cluster 9) contained only one OTU affiliated with the order Bacillales. Interestingly, this cluster integrated all three molecular levels, indicating that this single OTU drives the expression level of genes related to the sterol biosynthetic process in shoots (4 out of 58 genes, Dataset S4*F*), root accumulation of fructofuranose and glucopyranose, and exudation of 12 acylsugars (both acylsucroses and acylglucoses) esterified with acyl chains of various length.

Bacterial Reprogramming of Acylsugar Metabolism and Exudation. In order to test the SIREM model predicted in the SOM clusters 11

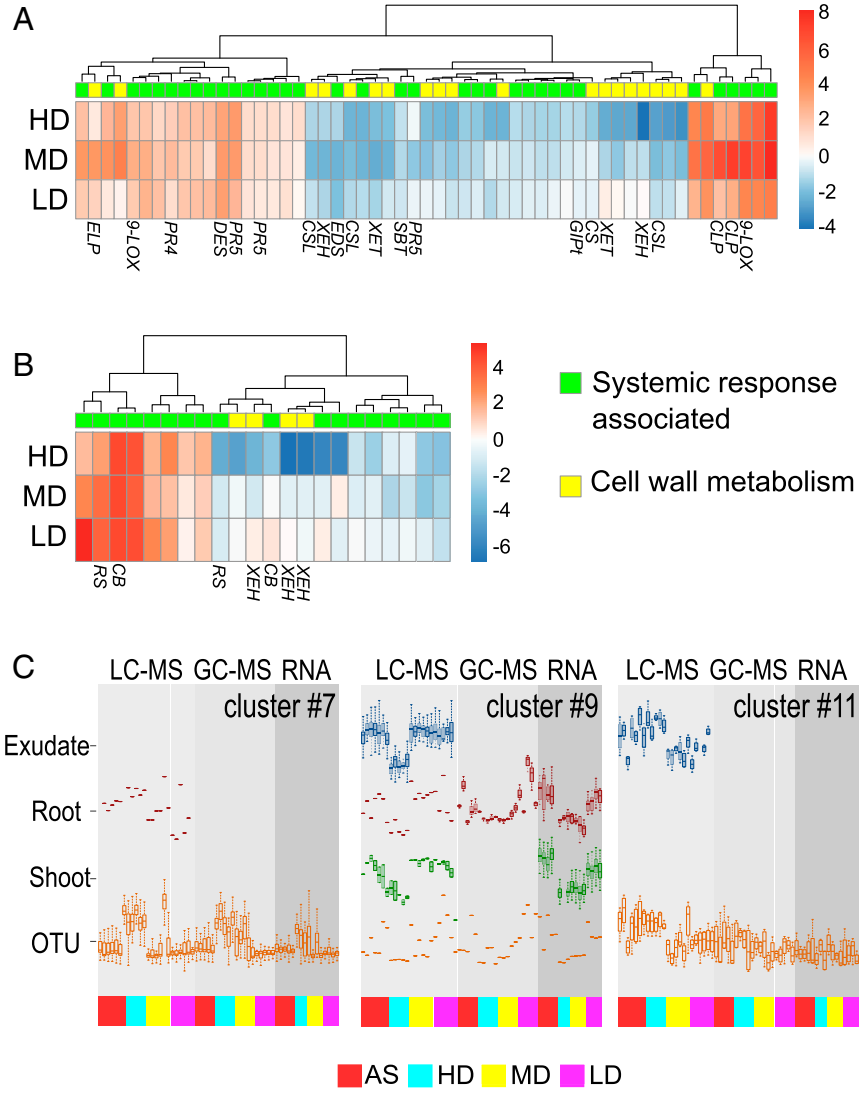

Fig. 5. Integration of SIREM-associated data. Heat maps representing the expression of known systemic response-associated genes (green) and those related to cell wall biosynthesis (yellow) expressed in (*A*) shoots and (*B*) roots significantly regulated by local-side root microbiome. Induced (red to white) and repressed (white to blue) genes are depicted as log2 (fold changes) relative to plants AS treated. *9-LOX*, 9-lipoxygenase; *CLP*, chitinase; *CSL*, cellulose synthase-like protein; *XEH*, xyloglucan endotransglucosylase-hydrolase; *XET*, xyloglucan endo-transglycosylase; *CS*, cellulose synthase; *GlPt*, glycerol-3-phosphate transporter; *PR5*, pathogen-induced protein 5; *SBT*, subtilisin-like protease; *EDS*, enhanced disease resistance-like protein; *DES*, divinyl ether synthase; *PR4*, pathogen-induced protein 4; *ELP*, extensin-like protein; *CB*, calcium-binding protein; *RS*, riboflavin biosynthesis protein. The gene annotations and numerical values can be found in Dataset S4 *B* and *E*. (*C*) Selected SOM clusters representing integrated data (i.e., microbiome, transcriptomics, and metabolomics). The dataset was filtered to include variables exhibiting significant root microbiome effects (ANOVA *P* value ≤0.05). Boxplots for the variables mapped to three SOM clusters. The OTU accumulation in these clusters was enriched in a specific bacterial group; clusters 7 and 11 accumulated OTUs related to Pseudomonadales, while cluster 9 accumulated one OTU related to Bacillales. The complete set of SOM clusters can be found in *SI Appendix*, Fig. S15 and the SOM classification of integrated data can be found in Dataset S5.

Downloaded at University of Manitoba Libraries on April 6, 2020

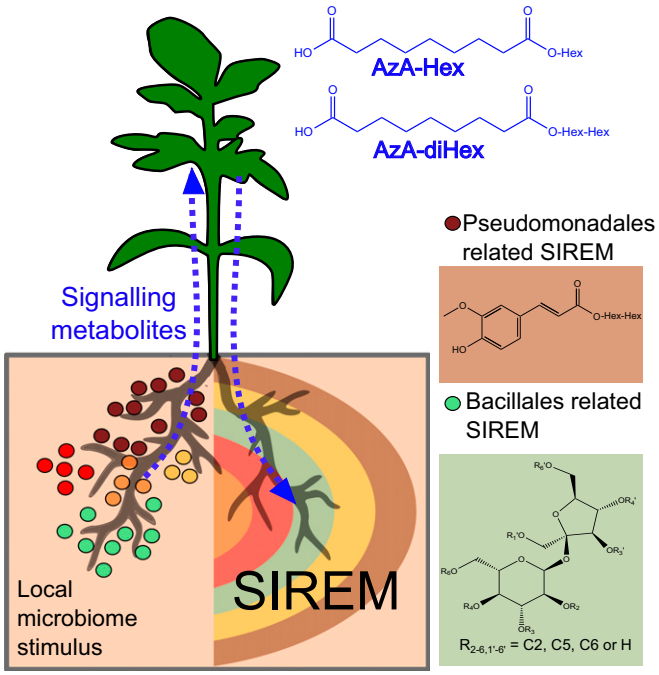

Fig. 6. Proposed model for the SIREM root–root signaling pathway resulting in systemic root exudation. Specific root bacterial populations colonizing the local root induce systemic root exudation of metabolites. For example, Pseudomonadales (brown circles) and Bacillales (green circles) are associated with secretion of ferulic acid hexose (structure in brown box) and the acylsucrose S4:19 (6, 6, 5, 2) (green box), respectively. Local root microbiome also induces accumulation of azelaic acid glycosides (mono- or diglycosylated; structures in blue) in plants. Azelaic acid glycosides are potential signaling metabolites (blue dashed arrows) triggering the SIREM process while the aglycone form of azelaic acid is a SIREM exudate component. In nature, SIREM represents a long-distance communication between unshared microhabitats of a plant rhizosphere. SIREM is triggered by a microbial population at a specific root zone; the signal likely reaches the shoot (e.g., AzA-Hex) and descends to unshared areas of the root, inducing systemic exudation that finally mediates rhizosphere interactions.

and 9, we treated plants with *Pseudomonas fluorescens* SBW25 and *Bacillus subtilis* 3610 in the local side and examined exudate composition collected from the systemic-side roots. While the overall metabolic profile did not change significantly following the treatment with individual bacterial strains (*SI Appendix*, Fig. S15), two isomers of the acylsugars S4:17 were significantly enriched in the systemic-side exudate of plants treated with *B. subtilis* 3610 as compared to the local side of the same plants, as well as to plants treated with *P. fluorescens* SBW25 (*SI Appendix*, Fig. S16). The acylsugar S4:16 showed a similar pattern, which was not statistically significant (*SI Appendix*, Fig. S17). The higher accumulation of these metabolites in the exudates from the systemic side of plants treated with *B. subtilis* 3610 corroborates the prediction of cluster 9; however, cluster 11 prediction was not supported by the inoculation of *P. fluorescens* SBW25.

To further examine the impact of specific bacteria on the systemic-side root response we analyzed the expression of the four known acylsugars acyltransferases (*ASATs*: *ASAT1*, *ASAT2*, *ASAT3*, and *ASAT4*), reported to catalyze acylations of acylsucroses in tomato glandular trichomes (28). While *B. subtilis* 3610 had no effect on these four *ASATs*' expression, *P. fluorescens* SBW25 significantly induced *ASAT4* expression (Solyc01g105580) in systemic-side roots as compared to roots of control plants (*SI Appendix*, Fig. S18). These results suggested that the *B. subtilis* 3610 strain induces exudate changes in acylsucroses through other, yet unexplored *ASAT* genes. Thus, we examined the expression level of 42 tomato acyltransferases genes belonging to the same phylogenetic clades (of the four characterized ASATs) and found that 15 of them were significantly induced in systemic-side roots of plants locally inoculated with the *B. subtilis* 3610 strain (*SI Appendix*, Fig. S19*A*). Interestingly, among the genes systemically induced in roots, Solyc01g105550 and Solyc01g105590 are close homologs of *Sl-ASAT4* (71% and 66% identical at the amino acid level; *SI Appendix*, Fig. S19*B*). The Sl-ASAT4 enzyme is responsible for making tetraacylated acylsucroses in tomato trichomes by acetylating triacylsucroses using acetyl-CoA (27). These two Sl-ASAT4 homologs are candidate enzymes for biosynthesis of tetraacylsucroses in tomato roots. If so, this finding supports the significant increase of the tetraacylsucroses S4:17 (2, 5, 5, 5) during SIREM of plants colonized by *B. subtilis*.

Discussion

The rhizosphere effect, i.e., the phenomenon of boosting microbial activity close to plant roots, has been studied over a century (43). This microbial enrichment was suggested to occur following root exudation, and specific microbes thrive in the rhizosphere according to the chemical dynamics of root exudates (44, 45). While systemic modification of plant metabolism following microbial colonization on roots or shoots was demonstrated aboveground (46, 47), systemic and comprehensive changes in root secondary metabolite exudation following local root colonization was not demonstrated to date. Here we show that tomato plants exude a mixture of metabolites, including acylsugars, steroidal glycoalkaloids, hydroxycinnamic acid derivatives, and organic acids in a root systemic manner. Moreover, we found that chemical composition of the systemic exudation is effected by specific microbial taxa established on local roots. In the case of *B. subtilis*, it induced a specific increase in acylsucrose exudation by the systemic-side root. This result validated our SIREM-model prediction, suggesting that bacteria related to the Bacillales order correlates with induced root exudation of acylsugars esterified with acyl chains of various lengths.

Acylsugars metabolites represented one of the major chemical classes induced in the tomato root exudation following SIREM. It included a total of 33 different metabolites among them acylsucroses and acylglucoses. Up to this study, acylsugar secondary metabolites have merely been reported to accumulate in aboveground organs, particularly leaf glandular trichomes, acting as insecticides and fungicides (48). In fact, leaf glandular trichomes of solanaceae family plants produce more than a hundred different acylsugars (31). The acylglucoses G2:12 (6, 6) detected in tomato exudates (Dataset S2*A*) were previously detected in leaf trichomes of *Datura metel*, a different Solanaceae species (49). It was suggested that the diversity of the acylsugar chemical class is either an accidental result of stochastic drift or due to enzymatic redundancy (31). Their detection in root tissue and modulation in exudates with large structural diversity suggests exclusive functions for this metabolite class in other interactions belowground, not merely protection against insects and fungi. Future research will therefore attempt to elucidate acylsugars' biosynthesis in roots of solanaceae plants and unravel the specific role of acylsugars' exudation in belowground interactions.

Plants integrate information regarding the availability of nutrients and biotic and abiotic external signals to adjust root development and plant–plant and plant–microbe interactions belowground (50). The work on SIREM highlighted aspects of plant systemic response, since we identified glycosylated forms of AzA and PIM as potential molecules involved in systemic root response to local bacterial colonization. In support of this, local AzA application triggered the systemic secretion of PIM, the SGA α-tomatine, as well as AzA itself. It is important to note that the AzA aglycone also induces SAR (36); however, it has not yet been proven to be an internal SAR mobile signal (37, 51). AzA exudation might also possess an additional role in mediating

Downloaded at University of Manitoba Libraries on April 6, 2020

plant–plant interactions, as this lipophilic molecule was recently associated with root growth under zinc-limiting conditions (52). From this perspective, root growth and root system architecture were suggested to be implicated in plant–microbe interactions (53).

Notably, spatial mapping of SIREM-associated metabolites pointed to their exclusive accumulation in specific root domains. Such demarcated metabolite localization likely results in root zone-confined exudation and consequently colonization of distinct microbial populations at specific root parts. We previously showed that *B. subtilis* colonize specifically the root elongation zone in *Arabidopsis*, using the TRIS (tracking root interactions system) microfluidics set-up (54). However, not only the colonization hotspots of the majority of root microbial populations are largely unknown, but also how root exudation of metabolites occurs in different root parts (i.e., main root, lateral roots, root hairs, root tip) is still not defined. Thus, we anticipate that cell type-specific localization of transporter proteins functioning in metabolite exudation is vastly important in SIREM, as programmed spatial and temporal secretion of particular metabolites is likely crucial for root interaction with certain microbial populations.

Chemical diversity is a major factor providing the means for plant growth and population fitness in changing environments (55). However, the metabolic repertoires in the roots and in the rhizosphere are often overlooked due to the challenge in studying the root system in natural settings. Following the findings in this study we anticipate that the metabolic composition associated with SIREM is likely a vital feature of belowground interactions. In this process, microbial stimuli occur locally in roots and in response, exudation in other parts of the root system, "conditions" the rhizosphere environment (Fig. 6). Especially in very large root systems such as in trees, a systemic signal that alerts the various parts of the root system following microbial colonization in one root location is highly pertinent.

Materials and Methods

Experimental details including citations are provided in *SI Appendix*.

Split-Root Hydroponics System and Sample Collection. A detailed description of the growth conditions of split-root tomato and the hydroponics system is provided in *SI Appendix, SI Materials and Methods*. Briefly, 14-d-old plants were incubated in the hydroponics set-up for 7 d before exchanging the medium to sterile distilled water in the systemic side. Likewise, the local side was refilled with: 1) a manipulated microbial community (i.e., a soil suspension prepared as described in *SI Appendix, SI Materials and Methods*); 2) autoclaved soil suspension, coded as AS (10% soil wt/vol); and 3) sterile distilled water. Local-side roots were used for microbiome analysis. Shoot, systemic-side root, and systemic-side exudate samples were prepared for metabolomic and for transcriptomic analyses.

Root Colonization and Microbiome Analysis. Microbial communities were obtained using the dilution-to-extinction approach (26) of a natural sandy loam. Sieved soil was serially diluted by 10^2-, 10^4-, and 10^6-fold in AS, leading to HD, MD, and LD microbial communities, respectively. Detailed steps for DNA extraction of local-side root microbiome, PCR with barcoded primers targeting the V4 region of bacterial 16S rRNA genes (515F and 806R), and Illumina MiSeq sequencing are in *SI Appendix, SI Materials and Methods*.

Metabolomics Analysis. The protocols used for the high-resolution mass spectrometry and the gas chromatography mass spectrometry are described thoroughly in *SI Appendix, SI Materials and Methods*.

Data Availability. Raw 16S rRNA amplicon-seq and RNA-seq reads were submitted to National Center for Biotechnology Information. UPLC-MS raw data were submitted to MetaboLights.

All other methods are described in *SI Appendix, SI Materials and Methods*.

ACKNOWLEDGMENTS. This work was supported by the Israel Ministry of Science and Technology (Grant 3-14297). E.K. was supported by the Israel Ministry of Absorption and the Weizmann Institute Faculty of Biochemistry Dean Fellowship. A.A. is the incumbent of the Peter J. Cohn Professorial Chair. We thank Georg Jender (Boyce Thompson Institute) for valuable comments on the manuscript. We are grateful to Guy Shmul, Gilad Jakoby, and Tamir Klein (Weizmann Institute of Science) for help with nutrient analysis.

1. D. S. Lundberg *et al.*, Defining the core Arabidopsis thaliana root microbiome. *Nature* **488**, 86–90 (2012).
2. S. Herrera Paredes, S. L. Lebeis, Giving back to the community: Microbial mechanisms of plant–soil interactions. *Funct. Ecol.* **30**, 1043–1052 (2016).
3. M. Ofek-Lalzar *et al.*, Niche and host-associated functional signatures of the root surface microbiome. *Nat. Commun.* **5**, 4950 (2014).
4. K. Schlaeppi, N. Dombrowski, R. G. Oter, E. Ver Loren van Themaat, P. Schulze-Lefert, Quantitative divergence of the bacterial root microbiota in Arabidopsis thaliana relatives. *Proc. Natl. Acad. Sci. U.S.A.* **111**, 585–592 (2014).
5. D. Bulgarelli *et al.*, Structure and function of the bacterial root microbiota in wild and domesticated barley. *Cell Host Microbe* **17**, 392–403 (2015).
6. J. D. Bever, T. G. Platt, E. R. Morton, Microbial population and community dynamics on plant roots and their feedbacks on plant communities. *Annu. Rev. Microbiol.* **66**, 265–283 (2012).
7. H. P. Bais, T. L. Weir, L. G. Perry, S. Gilroy, J. M. Vivanco, The role of root exudates in rhizosphere interactions with plants and other organisms. *Annu. Rev. Plant Biol.* **57**, 233–266 (2006).
8. J. Rajniak *et al.*, Biosynthesis of redox-active metabolites in response to iron deficiency in plants. *Nat. Chem. Biol.* **14**, 442–450 (2018).
9. I. A. Stringlis *et al.*, MYB72-dependent coumarin exudation shapes root microbiome assembly to promote plant health. *Proc. Natl. Acad. Sci. U.S.A.* **115**, E5213–E5222 (2018).
10. T. Rudrappa, K. J. Czymmek, P. W. Paré, H. P. Bais, Root-secreted malic acid recruits beneficial soil bacteria. *Plant Physiol.* **148**, 1547–1556 (2008).
11. D. L. Jones, C. Nguyen, R. D. Finlay, Carbon flow in the rhizosphere: Carbon trading at the soil-root interface. *Plant Soil* **321**, 5–33 (2009).
12. R. C. P. Kuijken, J. F. H. Snel, M. M. Heddes, H. J. Bouwmeester, L. F. M. Marcelis, The importance of a sterile rhizosphere when phenotyping for root exudation. *Plant Soil* **387**, 131–142 (2015).
13. H. Massalha, E. Korenblum, D. Tholl, A. Aharoni, Small molecules below-ground: The role of specialized metabolites in the rhizosphere. *Plant J.* **90**, 788–807 (2017).
14. E. Oburger, H. Schmidt, New methods to unravel rhizosphere processes. *Trends Plant Sci.* **21**, 243–255 (2016).
15. N. Strehmel, C. Böttcher, S. Schmidt, D. Scheel, Profiling of secondary metabolites in root exudates of Arabidopsis thaliana. *Phytochemistry* **108**, 35–46 (2014).
16. V. Venturi, C. Keel, Signaling in the rhizosphere. *Trends Plant Sci.* **21**, 187–198 (2016).
17. P. Pétriacq *et al.*, Metabolite profiling of non-sterile rhizosphere soil. *Plant J.* **92**, 147–162 (2017).
18. T. E. A. Cotton *et al.*, Metabolic regulation of the maize rhizobiome by benzoxazinoids. *ISME J.* **13**, 1647–1658 (2019).
19. P. Brinker, M. C. Fontaine, L. W. Beukeboom, J. Falcao Salles, Host, symbionts, and the microbiome: The missing tripartite interaction. *Trends Microbiol.* **27**, 480–488 (2019).
20. S. Okamoto, H. Shinohara, T. Mori, Y. Matsubayashi, M. Kawaguchi, Root-derived CLE glycopeptides control nodulation by direct binding to HAR1 receptor kinase. *Nat. Commun.* **4**, 2191 (2013).
21. A. Poitout *et al.*, Responses to systemic nitrogen signaling in Arabidopsis roots involve *trans*-Zeatin in shoots. *Plant Cell* **30**, 1243–1257 (2018).
22. C. M. J. Pieterse *et al.*, Induced systemic resistance by beneficial microbes. *Annu. Rev. Phytopathol.* **52**, 347–375 (2014).
23. G. A. Beattie, Metabolic coupling on roots. *Nat. Microbiol.* **3**, 396–397 (2018).
24. J. Sasse, E. Martinoia, T. Northen, Feed your friends: Do plant exudates shape the root microbiome? *Trends Plant Sci.* **23**, 25–41 (2018).
25. A. Singh, G.-H. Lim, P. Kachroo, Transport of chemical signals in systemic acquired resistance. *J. Integr. Plant Biol.* **59**, 336–344 (2017).
26. J. D. van Elsas *et al.*, Microbial diversity determines the invasion of soil by a bacterial pathogen. *Proc. Natl. Acad. Sci. U.S.A.* **109**, 1159–1164 (2012).
27. A. L. Schilmiller, A. L. Charbonneau, R. L. Last, Identification of a BAHD acetyltransferase that produces protective acyl sugars in tomato trichomes. *Proc. Natl. Acad. Sci. U.S.A.* **109**, 16377–16382 (2012).
28. P. Fan *et al.*, In vitro reconstruction and analysis of evolutionary variation of the tomato acylsucrose metabolic network. *Proc. Natl. Acad. Sci. U.S.A.* **113**, E239–E248 (2016).
29. A. Schilmiller *et al.*, Mass spectrometry screening reveals widespread diversity in trichome specialized metabolites of tomato chromosomal substitution lines. *Plant J.* **62**, 391–403 (2010).
30. B. Ghosh, T. C. Westbrook, A. D. Jones, Comparative structural profiling of trichome specialized metabolites in tomato (*Solanumlycopersicum*) and *S. habrochaites*: Acylsugar profiles revealed by UHPLC/MS and NMR. *Metabolomics* **10**, 496–507 (2014).
31. G. D. Moghe, B. J. Leong, S. M. Hurney, A. Daniel Jones, R. L. Last, Evolutionary routes to biochemical innovation revealed by integrative analysis of a plant-defense related specialized metabolic pathway. *eLife* **6**, e28468 (2017).
32. L. Zacarés *et al.*, Induction of p-coumaroyldopamine and feruloyldopamine, two novel metabolites, in tomato by the bacterial pathogen Pseudomonas syringae. *Mol. Plant Microbe Interact.* **20**, 1439–1448 (2007).
33. S. Mönchgesang *et al.*, Natural variation of root exudates in Arabidopsis thaliana-linking metabolomic and genomic data. *Sci. Rep.* **6**, 29033 (2016).

Downloaded at University of Manitoba Libraries on April 6, 2020

34. M. Itkin *et al.*, GLYCOALKALOID METABOLISM1 is required for steroidal alkaloid glycosylation and prevention of phytotoxicity in tomato. *Plant Cell* **23**, 4507–4525 (2011).
35. J. Vicente *et al.*, Role of 9-lipoxygenase and α-dioxygenase oxylipin pathways as modulators of local and systemic defense. *Mol. Plant* **5**, 914–928 (2012).
36. H. W. Jung, T. J. Tschaplinski, L. Wang, J. Glazebrook, J. T. Greenberg, Priming in systemic plant immunity. *Science* **324**, 89–91 (2009).
37. K. Yu *et al.*, A feedback regulatory loop between G3P and lipid transfer proteins DIR1 and AZI1 mediates azelaic-acid-induced systemic immunity. *Cell Rep.* **3**, 1266–1278 (2013).
38. N. M. Cecchini, K. Steffes, M. R. Schläppi, A. N. Gifford, J. T. Greenberg, Arabidopsis AZI1 family proteins mediate signal mobilization for systemic defence priming. *Nat. Commun.* **6**, 7658 (2015).
39. M. Zoeller *et al.*, Lipid profiling of the Arabidopsis hypersensitive response reveals specific lipid peroxidation and fragmentation processes: Biogenesis of pimelic and azelaic acid. *Plant Physiol.* **160**, 365–378 (2012).
40. K. Gruner, T. Griebel, H. Návarová, E. Attaran, J. Zeier, Reprogramming of plants during systemic acquired resistance. *Front. Plant Sci.* **4**, 252 (2013).
41. H. Dong, S. V. Beer, Riboflavin induces disease resistance in plants by activating a novel signal transduction pathway. *Phytopathology* **90**, 801–811 (2000).
42. R. Mittler, E. Blumwald, The roles of ROS and ABA in systemic acquired acclimation. *Plant Cell* **27**, 64–70 (2015).
43. L. Hiltner, Über neuere erfahrungen und probleme auf dem gebiete der bodenbakteriologie unter besonderer berücksichtigung der gründüngung und brache. *Arb der Dtsch Landwirtsch Gesellschaft* **98**, 59–78 (1904).
44. K. Zhalnina *et al.*, Dynamic root exudate chemistry and microbial substrate preferences drive patterns in rhizosphere microbial community assembly. *Nat. Microbiol.* **3**, 470–480 (2018).
45. J. M. Chaparro *et al.*, Root exudation of phytochemicals in Arabidopsis follows specific patterns that are developmentally programmed and correlate with soil microbial functions. *PLoS One* **8**, e55731 (2013).
46. D. W. Etalo, J. S. Jeon, J. M. Raaijmakers, Modulation of plant chemistry by beneficial root microbiota. *Nat. Prod. Rep.* **35**, 398–409 (2018).
47. E. Korenblum, A. Aharoni, Phytobiome metabolism: Beneficial soil microbes steer crop plants' secondary metabolism. *Pest Manag. Sci.* **75**, 2378–2384 (2019).
48. V. T. Luu *et al.*, *O*-acyl sugars protect a wild tobacco from both native fungal pathogens and a specialist herbivore. *Plant Physiol.* **174**, 370–386 (2017).
49. R. R. King, L. A. Calhoun, 6 2,3-Di-O- and 1,2,3-tri-O-acylated glucose esters from the glandular trichomes of Datura metel. *Phytochemistry* **27**, 3761–3763 (1988).
50. L. Mommer, J. Kirkegaard, J. van Ruijven, Root-root interactions: Towards A rhizosphere framework. *Trends Plant Sci.* **21**, 209–217 (2016).
51. N. M. Cecchini *et al.*, Underground azelaic acid-conferred resistance to Pseudomonas syringae in Arabidopsis. *Mol. Plant Microbe Interact.* **32**, 86–94 (2019).
52. N. Bouain *et al.*, Natural allelic variation of the AZI1 gene controls root growth under zinc-limiting condition. *PLoS Genet.* **14**, e1007304 (2018).
53. S. A. Micallef, M. P. Shiaris, A. Colón-Carmona, Influence of Arabidopsis thaliana accessions on rhizobacterial communities and natural variation in root exudates. *J. Exp. Bot.* **60**, 1729–1742 (2009).
54. H. Massalha, E. Korenblum, S. Malitsky, O. H. Shapiro, A. Aharoni, Live imaging of root-bacteria interactions in a microfluidics setup. *Proc. Natl. Acad. Sci. U.S.A.* **114**, 4549–4554 (2017).
55. J. K. Weng, R. N. Philippe, J. P. Noel, The rise of chemodiversity in plants. *Science* **336**, 1667–1670 (2012).

Downloaded at University of Manitoba Libraries on April 6, 2020